European Review for Medical and Pharmacological Sciences 2020; 24: 4412-4419

A relationship between MAPK/ERK pathway expression and neuronal apoptosis in rats with white matter lesions

Y. GUO[1], C. LIU[2], J. ZHANG[1], B.-B. TIAN[1], L. WANG[1], G.-K. LIU[1], Y. LIU[1]

[1]Department of Anesthesiology, Dongzhimen Hospital Beijing University of Chinese Medicine, Beijing, China
[2]Department of Emergency, Beijing Friendship Hospital, Capital Medical University, Beijing, China

Abstract. – OBJECTIVE: The aim of this study was to explore the association between the expression of mitogen-activated protein kinase (MAPK)/extracellular regulated protein kinase (ERK) pathway and neuronal apoptosis in rats with white matter lesions (WML).

MATERIALS AND METHODS: Sprague-Dawley (SD) rats were selected as the research objects. Rat models of ischemic WML were established by bilateral common carotid artery ligation. Subsequently, brain tissues were collected from rats in sham operation group and WML group, respectively. Hematoxylin-eosin (HE) staining assay was conducted to observe the pathological changes in white matters (WMs) (callosum, internal capsule, and optic nerve) and apoptotic cells in brain tissues. The protein expression levels of phosphorylated ERK (p-ERK) and ERK, phosphorylated MAPK (p-MAPK), and MAPK in tissues were measured by Western blotting. Immunohistochemistry was employed to detect the expression levels of p-ERK, ERK, p-MAPK, and MAPK in brain tissues of the two groups. Next, nerve cells were isolated from rats with WML as research objects. The phosphorylation of the MAPK/ERK pathway was suppressed using PD03259019 (a chemical drug, hereafter referred to as PD). Then, the changes in the protein expressions of apoptosis proteins B-cell lymphoma 2 (Bcl-2) and Bcl-2-associated X protein (Bax) were determined before and after MAPK/ERK pathway inhibition. Meanwhile, changes in the messenger ribonucleic acid (mRNA) expression levels were detected *via* real-time fluorescent quantitative polymerase chain reaction (PCR), and changes in apoptosis were observed.

RESULTS: HE staining revealed that in sham operation group, WMs had normal structure and intact morphology. The cells were regularly arranged, with little apoptosis of the nuclei in the center. However, there were abnormally arranged nerve cells, loose cortical structure, swollen cells, aberrant nuclear membrane, pyknosis, signs of cell degeneration and necrosis, apoptotic cells filled most of the field of vision, and relatively evident lesions in WML group. Besides, WML group exhibited significantly up-regulated expressions of p-ERK and p-MAPK, as well as basically unchanged expressions of ERK and MAPK ($p<0.05$). After PD was added for 1 d, 2 d, and 3 d, the MAPK/ERK pathway was repressed, which was the most significantly at 3 d. Furthermore, the anti-apoptotic phenotype of neurons was detected, which was more pronounced at 3 d ($p<0.05$).

CONCLUSIONS: Rats with WML exhibited elevated MAPK/ERK activity and evident apoptosis. After inhibiting the phosphorylation site of MAPK/ERK in rat neuronal cells, the expression of pro-apoptotic protein decreased, and the apoptosis was relieved. In rats with WML, neuronal apoptosis is promoted by activating the MAPK/ERK pathway, thus worsening the condition.

Key Words:
White matter lesions (WML), MAPK/ERK pathway, Apoptosis.

Introduction

White matter lesions (WML) is caused by chronic cerebral hypoperfusion even in the absence of cerebral infarction, which develops with age. The risk for WML rises in patients with arterial hypertension, diabetes mellitus (DM) or cardiovascular diseases[1]. WML can be detected in the brain of 27-87% of patients aged over 65 years old, which has also been proved to be closely associated with weakened cognitive ability[2]. WML is correlated with diseases affecting cerebral small blood vessels (e.g., radioactive lacunar infarction). Meanwhile, it is often found

Corresponding Authors: Yang Liu, MD; e-mail: daveqiliu@163.com
Guokai Liu MD; e-mail: batianzh7962969@163.com

in patients with stroke, and is regarded as one of the most common causes of vascular cognitive impairment and dementia[3-7]. Actually, WML is a core pathology of Binswanger disease (a kind of vascular dementia). Partial WML can be used to explain Alzheimer's disease[5-7]. WML can also be detected *via* diffusion weighted imaging and diffusion tensor imaging techniques[8]. In addition, the pathophysiology of ischemic injury in white matters (WMs) differs greatly from that in gray matters. In addition to Wallerian degeneration, WM injury can be independently induced by degeneration secondary to neuronal damage[9,10]. Given this, some researchers have emphasized the importance of "comprehensive brain protection" to protect gray matters and WMs from acute cerebral ischemia[9,11]. Preoperative WML is a severe and important risk factor for postoperative cognitive dysfunction (POCD) in humans[12-14]. Diabetes mellitus and brain, heart or vascular diseases are common risk factors for WML and POCD[15,16]. Meanwhile, it has been reported that in the case of WML, microglial cells are activated. This may produce excessive reactive oxygen species and pro-inflammatory cytokines and activate mitogen-activated protein kinase (MAPK) signal transduction, eventually aggravating WML[17,18]. Therefore, exploring the correlation between WML and the activation of MAPK/extracellular regulated protein kinase (ERK) pathway after WML may be conducive to the treatment of WML.

Materials and Methods

Materials

Sprague-Dawley (SD) rats (fed in our hospital), rat-derived nerve cells B-35 [purchased from American Type Culture Collection (ATCC) cell bank (Manassas, VA, USA)]; quantitative polymerase chain reaction (PCR) kit (Roche, Basel, Switzerland); B-cell lymphoma 2 (Bcl-2) and Bcl-2-associated X protein (Bax) antibodies (Santa Cruz Biotechnology, Santa Cruz, CA, USA); PD inhibitor (Shanghai Jingke Chemical Biology, Shanghai, China); hematoxylin-eosin (HE) staining reagent (Beyotime, Shanghai, China); protein concentration assay kit (Elabscience, Wuhan, China) and TRIzol (Aidlab, Beijing, China).

Research Objects and Grouping

Female SD rats were used as research objects for *in vivo* experiments. All rats were divided into two groups based on the presence or absence of carotid artery ligation, including sham operation group (n=10) and WML group (n=10). PD was prepared with dimethyl sulfoxide (DMSO), and rat nerve cells were divided into DMSO group and PD group. Meanwhile, PD group was subdivided into 1 d group, 2 d group, and 3 d group. This investigation was approved by the Ethics Committee of Dongzhimen Hospital Beijing University of Chinese Medicine.

Establishment of Rat Models of WML

The rats were first placed on an operating table and anesthetized with 5% chloral hydrate (0.01 mL/g body weight; Wuhan Hengwo Technology Co., Ltd., Wuhan, China). In WML group, the right common carotid artery of rats was permanently ligated under anesthesia. Then, the rats were put in a sealed 3 L container that was partially immersed in a water bath at 36°C, followed by exposure to 8% wet oxygen (8% O_2 and 92% N_2) at a flow rate of 3 L/min for 1 h. After hypoxia, the rats were put back to the cages. Next, behavioral changes in rats of the two groups were observed. Rats in sham operation group did not undergo ligation of carotid and other treatments, and the right carotid artery was only threaded.

Morris Water Maze Experiment

At the beginning of the experiment, rats were placed on a platform for 20 s to be directed to the maze. Next, the tail of rats was gently lowered to one of the three positions (located in the center of the wall of the different quadrants without platforms) in the pool facing the wall. Meanwhile, a digital tracking system was started to record the test. The maximum swimming time was set as 60 s, and the swimming trajectory of rats was recorded. To check the spatial reference memory, a probe test was performed at 24 h after last detection. During the test, the rats were allowed to fall into the pool and swim for 1 min. 30 min after the probe test, a visual cue test was conducted to assess sensorimotor ability and motivation.

Hematoxylin and Eosin (HE) Staining

The rats were first killed after anesthesia with chloral hydrate. Brain tissues around the ventricle were taken, dissected, thoroughly washed and dissolved, fixed with 4% paraformaldehyde, and embedded in paraffin. Next, paraffin blocks were coronally sectioned (10 μm in thickness) from the genus of the callosum to the end of the dorsal

hippocampus. The sections were pre-heated at 65°C overnight on the day before the experiment. At the beginning of the experiment, the sections were deparaffinized in xylene tanks with three concentrations. After dehydration by ethanol at 5 gradually increasing concentrations, the sections were gently washed with deionized water for 4 times, and dried in air. Then, the tissues were spread on a sterile glass slide and placed above the alcohol lamp flame for 15-30 s. Next, they were added dropwise with eosin Y staining solution and let stand for 3 min for cell plasma staining. After that, the staining solution was diluted with distilled water to terminate the staining. Thereafter, stained tissue samples were slowly washed with ethanol and added with methylene blue staining solution in drops for cell nucleus staining for 60 s. The staining was terminated using the same method as above. Lastly, the tissue samples were mounted for long-term preservation.

Tissue Protein Extraction and Western Blotting Analysis

After killing the rats, brain tissues were quickly taken out. Tissues around the ventricle were dissected and stored in equal parts at –80°C, which were thawed and taken out for next use. Subsequently, tissue lysis buffer was prepared and mixed with the tissues evenly, swirled for three times (15 s/time), and centrifuged at 14000 rpm/min for 40 min. Protein concentration was determined according to absorbance, and the samples were boiled for denaturation. Next, protein samples were separated *via* sodium dodecyl sulphate-polyacrylamide gel electrophoresis (SDS-PAGE) and transferred onto polyvinylidene difluoride (PVDF) membranes (Millipore, Billerica, MA, USA). Then, the membranes were incubated with Bcl-2 and Bax (1:2000) and anti-glyceraldehyde-3-phosphate dehydrogenase (GAPDH; 1:1000) primary antibodies at 4°C for 14 h. On the next day, the membranes were incubated with horseradish peroxidase (HRP)-labeled secondary antibodies (1:1000) for 1 h. After that, luminous solution was prepared at 1:1 and used for development. The analytical experimental results were saved.

Real-Time Reverse Transcription PCR

Total ribonucleic acids (RNAs) in brain tissues were extracted with TRIzol. Subsequently, extracted RNA was reversely transcribed into complementary deoxyribonucleic acids (cDNAs) using a reverse transcription system. The reverse transcription system (Roche, Basel, Switzerland) was added with RNAs and reagent 5, 6 and 7, and heated at 65°C for 10 min. After successively added with reagent 2, 3, 4, and 1, the mixture was heated at 50°C for 60 min and 85°C for 5 min to obtain cDNAs. The concentration of cDNAs was detected, and they were diluted to 500 ng/μL and added with buffer primer cDNAs and water to prepare into a general reaction system (20 μL in total). Glyceraldehyde 3-phosphate dehydrogenase (GAPDH) was used as an internal reference for Bcl-2 and Bax. For each sample, three replicates were set. Expression levels of genes were calculated by the $2^{-\Delta\Delta Ct}$ method. Primer sequences used in the experiment were as follows: Bax-F: TCCACCAAGAAGCTGAGCGAG; Bax-R: GTCCAGCCCATGATGGTTCT. Bcl-2-F: TTCTTTGAGTTCGGTGGGGTC; Bcl-2-R: TGCATATTTGTTTGGGGCAGG. GAPDH-F: ACAGCAACAGGGTGGTGGAC; GAPDH-R: TTTGAGGGTGCAGCGAACTT.

Cell Dosing

One day before the experiment, rat glial cells were inoculated into a 6-well plate and divided into DMSO group, 1 d group, 2 d group, and 3 d group. Multiple wells were set for each group. The number of cells inoculated was determined based on culture time. Next, PD (10 μM) and the medium (1.5 mL) were added, and the cell pellet was collected.

Statistical Analysis

Statistical Product and Service Solutions (SPSS) 17.0 (SPSS Inc., (Chicago, IL, USA) software was used for all statistical analysis. The *t*-test and single factor analysis were carried out when appropriate. $p<0.05$ was considered statistically significant.

Results

Behavioral Changes and Behavioral Test Results in Rats With WML

Rats in sham operation group had normal performance, while those in WML group exhibited limb shaking, dysphoria (in emotion), cyanosis (in skin), shortness of breath, hovering, and convulsions. Based on the water maze experiment, the memory capacity was overtly weakened, the swimming path was notably messy and had no rules, and the times of platform crossing were reduced in WML group when compared with sham operation group (Figure 1).

Morphological Changes in Nerve Cells Detected Via HE Staining

HE staining indicated that WM area in sham operation group was normal. Nerve cells exhibited a complete shape, and no brain edema and brain atrophy were observed by naked eyes. In WM area in WML group, the fibers were disorderly arranged, with vacuole-like changes in some fibers. Meanwhile, apoptosis was evident, and neutrophil infiltration was observed (Figure 2).

Changes in MAPK/ERK Pathway and Apoptosis After WML

The expression levels of phosphorylated ERK (p-ERK) and phosphorylated MAPK (p-MAPK) in WML group were significantly higher than those in sham operation group. However, no significant differences were observed in the expression levels of MAPK and ERK between the two groups. These results suggested that the MAPK/ERK pathway was activated after WML, and the expression of important proteins of the pathway was significantly high (Figure 3).

Relationship Between MAPK/ERK Pathway and Neuronal Apoptosis

After adding PD, MAPK/ERK began to be inactivated. Protein expressions decreased at 2 d, and the inhibition was the strongest at 3 d. Compared with DMSO group, the expression of apoptosis proteins in nerve cells was not significantly different in 1 d group. However, it was markedly reduced in 2 d and 3 d groups. The decrease was the most evident in 3 d group and prominent in 2 d group. QRCR results revealed that 2 d and 3 d groups showed significantly elevated expression of Bcl-2 and decreased expression of Bax. The above results suggested that neuronal apoptosis was attenuated after the MAPK/ERK pathway was repressed (Figure 4).

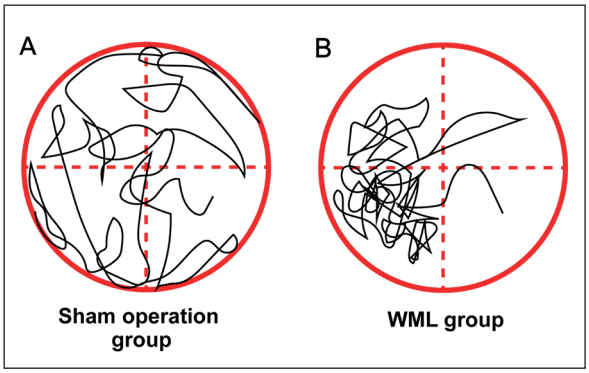

Figure 1. Results of behavioral test of rats after WML. **A,** Swimming path of rats in sham operation group is regular. **B,** Rats in WML group have disordered swimming path and decreased times of platform crossing.

Discussion

WML is an important neurological deficit commonly detected in premature infants with very low birth weight (VLBW). It accounts for 10% of cerebral palsy and 25-50% of cognitive/behavioral deficits in VLBW premature infants[19].

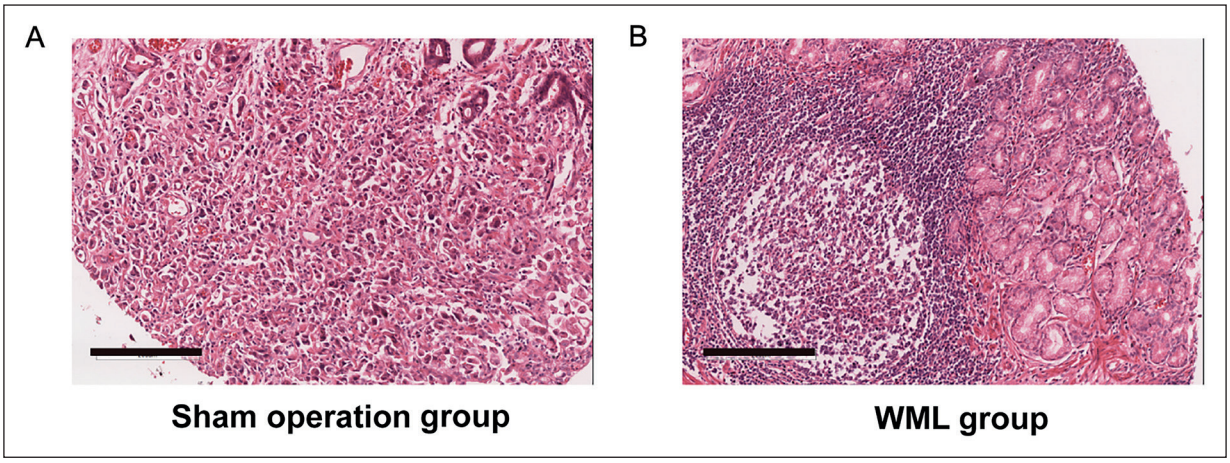

Figure 2. Pathological changes in WM area after WML. **A,** Nerve cells are relatively intact in sham operation group, with little necrotic cells. **B,** WML group has disordered arrangement of nerve fibers, swollen and deformed cells, infiltration of inflammatory cells and clearly increased apoptotic cells (magnification 4×).

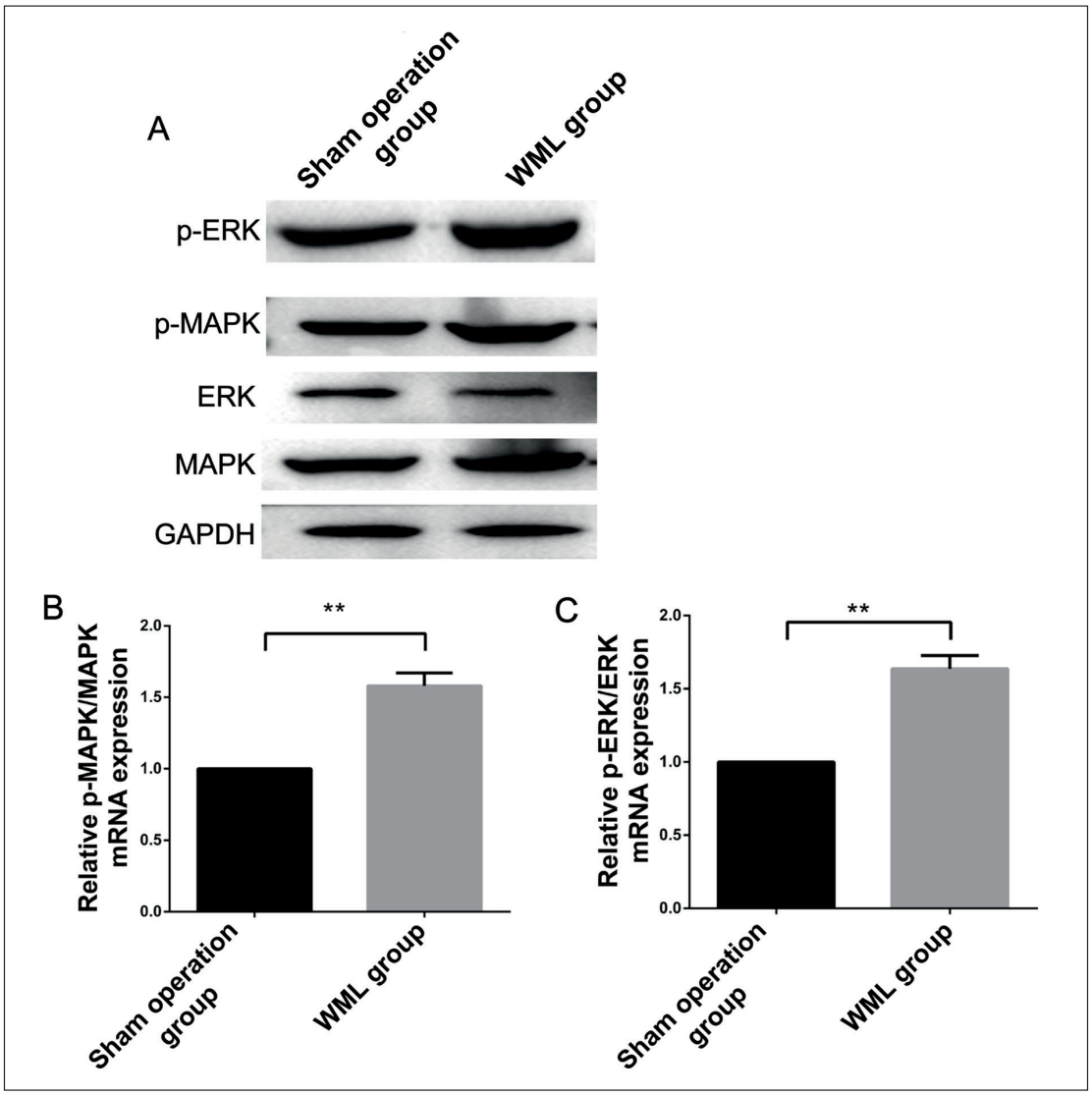

Figure 3. The MAPK/ERK pathway is activated in the case of WML**. A,** Compared with sham operation group, WML group exhibits remarkably raised p-MAPK and p-ERK expressions ($p<0.05$) and basically unchanged MAPK and ERK expressions. **B, C,** Expression levels of p-MAPK/MAPK and p-ERK/ERK are evidently up-regulated in WML group ($p<0.01$).

Zhang et al[20] have reported that 19.3% of surviving premature infants have cerebellar lesions. The pathogenesis of WML mainly involves cerebral hypoxia-ischemia (HI) injury-induced systemic inflammation and maternal or fetal infection. So far, there are little pharmacological drugs that can effectively alleviate brain damage in premature infants, promote rehabilitation, or minimize the severity of disability. HI and infection/inflammation are two major risk factors for WML in premature infants with VLBW[19,21,22]. However, clinical and experimental evidence has demonstrated that systemic infection or inflammation is insufficient to result in significant lesions of the central nervous system. Leviton and Gilles[23] have proved that maternal infection is critical to the progression of WML. To sum up, WML is a multifactorial process, in which HI injury and inflammation negatively impact immature brain at the same time.

The MAPK/ERK pathway is widely involved in every stage of the growth and development of cells, including cell proliferation, differentiation, migration, senescence, and apoptosis. Neurotroph-

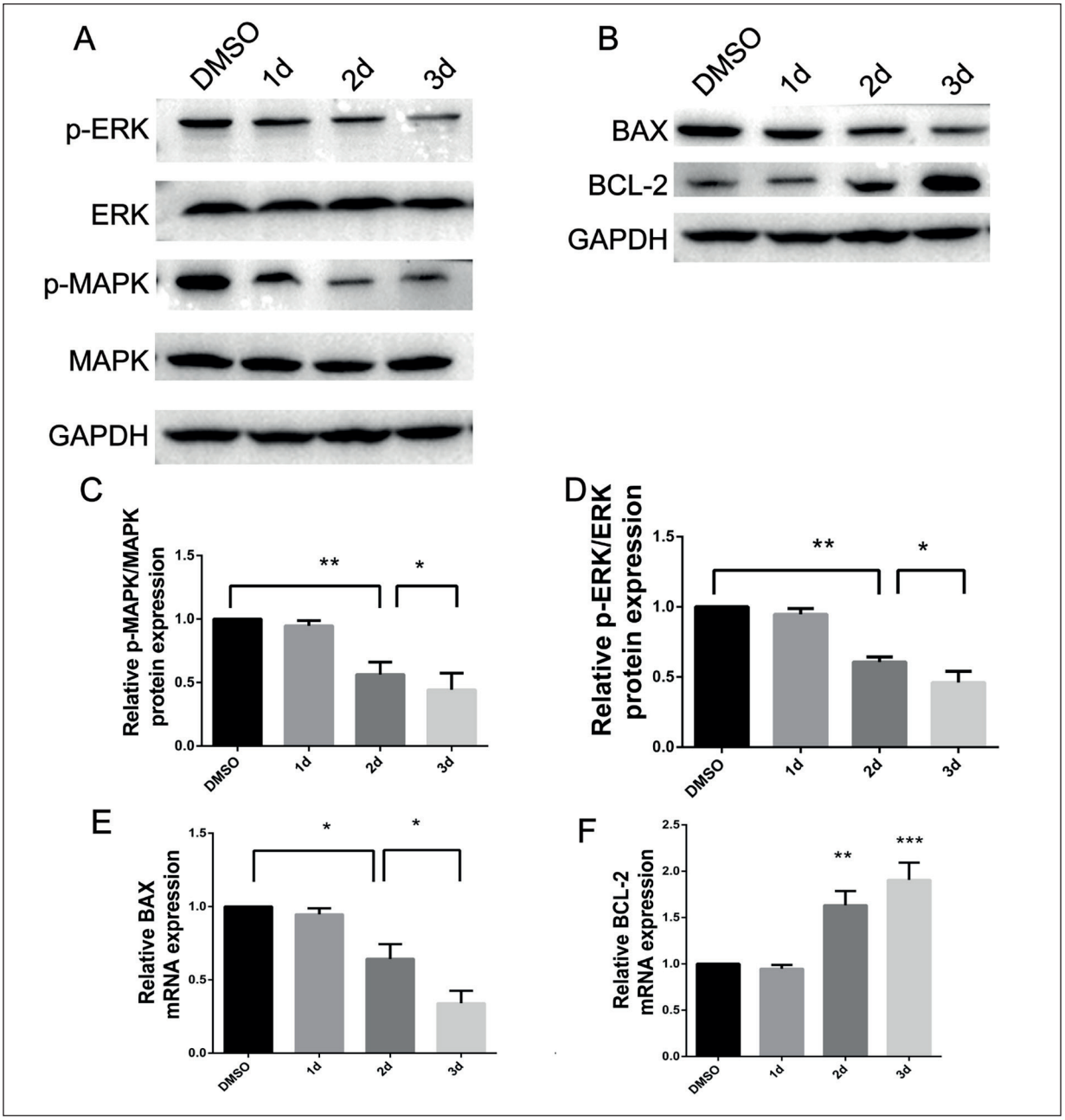

Figure 4. Apoptosis changes after inhibition of the MAPK/ERK pathway. **A,** Compared with DMSO group, PD exerts inhibitory function from 2 d, and the inhibitory effect is more significant at 3 d ($p<0.05$) **B,** Compared with DMSO group, 2 d and 3 d groups exhibits elevated Bcl-2 protein expression and lowered Bax protein expression, showing significant differences ($p<0.01$). **C, D,** Levels of p-ERK and p-MAPK display no significant differences between DMSO group and 1 d group, but overtly lower in 2 d and 3 d groups than those in DMSO group ($p<0.01$). **E, F,** In comparison with DMSO group, 2 d and 3 d groups have elevated Bcl-2 mRNA content and lowered Bax mRNA content ($p<0.01$).

ic factors from the brain can stimulate neural differentiation of human cord blood mesenchymal stem cells (MSCs) and the survival of differentiated cells through MAPK/ERK-dependent signaling pathways[24]. Suppression of the MAPK/ERK pathway has also been found associated with TNF-α-induced apoptosis of neuronal cell PC12[25]. Therefore, further exploring the relationship between MAPK/ERK pathway and apoptosis in patients with WML can more clearly explain the pathogen-

esis of WML, thereby providing a new method for its treatment in clinical practice.

In this study, rat models of WML were firstly constructed. Compared with sham operation group, the behaviors changed greatly in WML group. Transiently limb shaking, irritability, cyanosis, and tachypnea were observed. Water maze experiment showed that compared with sham operation group, WML group exhibited reduced memory, chaotic and irregular swimming path, and decreased times of platform crossing. HE staining results of the WM area demonstrated that in WML group, the nerve fibers were disordered, without rules. More cells had degeneration and necrosis, with vacuoles in some cells. Meanwhile, formed lesions were observed under a microscope. Furthermore, the expression levels of p-MAPA and p-AKT were significantly higher in WML group than those in sham operation group. However, no significant differences in the protein expression levels of MAPK and ERK were observed between sham operation group and WML group. PD acted on the phosphorylation site of proteins to inhibit the MAPK/ERK pathway in rat glial cells. At 1 d after dosing, PD exerted no evident inhibitory effect. However, its inhibitory effect was enhanced at 2 d and 3 d after dosing. The measurement of the protein and mRNA expressions of apoptosis-related proteins showed that the expression of Bcl-2 rose in 2 d and 3 d groups, while Bax expression declined. Such an increase or decrease was particularly evident in 3 d group, and the differences were statistically significant. *In vivo* experiments indicated that the MAPK/ERK pathway was activated, and the apoptosis increased in the case of WML. *In vitro* experiments uncovered that after inhibiting the MAPK/ERK pathway, the protein expression of Bax in nerve cells was significantly reduced, while that of Bcl-2 was elevated. Meanwhile, the anti-apoptotic effect was significant, indicating that the MAPK/ERK pathway could mediate the apoptosis of nerve cells after WML. In this study, the mechanism of MAPK/ERK pathway activation in WML was not investigated. Non-coding RNAs might be involved in the activation, which could serve as sites for targeted therapy.

Conclusions

Briefly, rats with WML showed elevated MAPK/ERK activity and evident apoptosis. After inhibiting the phosphorylation site of MAPK/ERK in rat neuronal cells, the expression of pro-apoptotic protein decreased, and the apoptosis was relieved. In rats with WML, neuronal apoptosis was promoted by activating the MAPK/ERK pathway, thus worsening the condition. Our study could provide a potential strategy in clinical treatment for WML.

Conflict of Interest

The Authors declare that they have no conflict of interests.

References

1) Otero-Ortega L, Gutierrez-Fernandez M, Ramos-Cejudo J, Rodriguez-Frutos B, Fuentes B, Sobrino T, Hernanz TN, Campos F, Lopez JA, Cerdan S, Vazquez J, Diez-Tejedor E. White matter injury restoration after stem cell administration in subcortical ischemic stroke. Stem Cell Res Ther 2015; 6: 121.
2) Longstreth WJ, Manolio TA, Arnold A, Burke GL, Bryan N, Jungreis CA, Enright PL, O'Leary D, Fried L. Clinical correlates of white matter findings on cranial magnetic resonance imaging of 3301 elderly people. The Cardiovascular Health Study. Stroke 1996; 27: 1274-1282.
3) Pantoni L, Garcia JH. Pathogenesis of leukoaraiosis: a review. Stroke 1997; 28: 652-659.
4) Schmidt R, Scheltens P, Erkinjuntti T, Pantoni L, Markus HS, Wallin A, Barkhof F, Fazekas F. White matter lesion progression: a surrogate endpoint for trials in cerebral small-vessel disease. Neurology 2004; 63: 139-144.
5) Pantoni L. Cerebral small vessel disease: from pathogenesis and clinical characteristics to therapeutic challenges. Lancet Neurol 2010; 9: 689-701.
6) Desmond DW. Cognition and white matter lesions. Cerebrovasc Dis 2002; 13 Suppl 2: 53-57.
7) Duncombe J, Kitamura A, Hase Y, Ihara M, Kalaria RN, Horsburgh K. Chronic cerebral hypoperfusion: a key mechanism leading to vascular cognitive impairment and dementia. Closing the translational gap between rodent models and human vascular cognitive impairment and dementia. Clin Sci (Lond) 2017; 131: 2451-2468.
8) Schmidt R, Grazer A, Enzinger C, Ropele S, Homayoon N, Pluta-Fuerst A, Schwingenschuh P, Katschnig P, Cavalieri M, Schmidt H, Langkammer C, Ebner F, Fazekas F. MRI-detected white matter lesions: do they really matter? J Neural Transm (Vienna) 2011; 118: 673-681.
9) Dewar D, Yam P, McCulloch J. Drug development for stroke: importance of protecting cerebral white matter. Eur J Pharmacol 1999; 375: 41-50.
10) Matute C. Glutamate and ATP signalling in white matter pathology. J Anat 2011; 219: 53-64.

11) Kubo K, Nakao S, Jomura S, Sakamoto S, Miyamoto E, Xu Y, Tomimoto H, Inada T, Shingu K. Edaravone, a free radical scavenger, mitigates both gray and white matter damages after global cerebral ischemia in rats. Brain Res 2009; 1279: 139-146.

12) Hatano Y, Narumoto J, Shibata K, Matsuoka T, Taniguchi S, Hata Y, Yamada K, Yaku H, Fukui K. White-matter hyperintensities predict delirium after cardiac surgery. Am J Geriatr Psychiatry 2013; 21: 938-945.

13) Maekawa K, Baba T, Otomo S, Morishita S, Tamura N. Low pre-existing gray matter volume in the medial temporal lobe and white matter lesions are associated with postoperative cognitive dysfunction after cardiac surgery. PLoS One 2014; 9: e87375.

14) Kant I, de Bresser J, van Montfort S, Slooter A, Hendrikse J. MRI Markers of neurodegenerative and neurovascular changes in relation to postoperative delirium and postoperative cognitive decline. Am J Geriatr Psychiatry 2017; 25: 1048-1061.

15) Feinkohl I, Winterer G, Pischon T. Diabetes is associated with risk of postoperative cognitive dysfunction: a meta-analysis. Diabetes Metab Res Rev 2017; 33. doi: 10.1002/dmrr.2884

16) Rundshagen I. Postoperative cognitive dysfunction. Dtsch Arztebl Int 2014; 111: 119-125.

17) Farkas E, Donka G, de Vos RA, Mihaly A, Bari F, Luiten PG. Experimental cerebral hypoperfusion induces white matter injury and microglial activation in the rat brain. Acta Neuropathol 2004; 108: 57-64.

18) Haddad JJ. Mitogen-activated protein kinases and the evolution of Alzheimer's: a revolutionary neurogenetic axis for therapeutic intervention? Prog Neurobiol 2004; 73: 359-377.

19) Vincer MJ, Allen AC, Joseph KS, Stinson DA, Scott H, Wood E. Increasing prevalence of cerebral palsy among very preterm infants: a population-based study. Pediatrics 2006; 118: e1621-e1626.

20) Zhang X, Yan Y, Tong F, Li CX, Jones B, Wang S, Meng Y, Muly EC, Kempf D, Howell L. Progressive assessment of ischemic injury to white matter using diffusion tensor imaging: a preliminary study of a Macaque model of stroke. Open Neuroimag J 2018; 12: 30-41.

21) Stoll BJ, Hansen NI, Adams-Chapman I, Fanaroff AA, Hintz SR, Vohr B, Higgins RD. Neurodevelopmental and growth impairment among extremely low-birth-weight infants with neonatal infection. JAMA 2004; 292: 2357-2365.

22) Wang LW, Lin YC, Wang ST, Yeh TF, Huang CC. Hypoxic/ischemic and infectious events have cumulative effects on the risk of cerebral palsy in very-low-birth-weight preterm infants. Neonatology 2014; 106: 209-215.

23) Leviton A, Gilles FH. Acquired perinatal leukoencephalopathy. Ann Neurol 1984; 16: 1-8.

24) Lim JY, Park SI, Oh JH, Kim SM, Jeong CH, Jun JA, Lee KS, Oh W, Lee JK, Jeun SS. Brain-derived neurotrophic factor stimulates the neural differentiation of human umbilical cord blood-derived mesenchymal stem cells and survival of differentiated cells through MAPK/ERK and PI3K/Akt-dependent signaling pathways. J Neurosci Res 2008; 86: 2168-2178.

25) Marques-Fernandez F, Planells-Ferrer L, Gozzelino R, Galenkamp KM, Reix S, Llecha-Cano N, Lopez-Soriano J, Yuste VJ, Moubarak RS, Comella JX. TNFalpha induces survival through the FLIP-L-dependent activation of the MAPK/ERK pathway. Cell Death Dis 2013; 4: e493.